Laboratory Observations of Shear Alfvén Waves Launched from a Small Source

D. Leneman, W. Gekelman, and J. Maggs
Department of Physics, University of California, Los Angeles, California 90095
(Received 14 July 1998)

Shear Alfvén waves with transverse scales of electron skin-depth size are launched with a dual-disk antenna in the Large Plasma Device at UCLA. The waves are studied in the kinetic and inertial regimes. The kinetic shear Alfvén wave is observed for the first time and exhibits predicted radial structure. The perpendicular propagation of the wave is also studied for the first time, and it is found to be backward in the inertial regime, as expected. The wave currents are calculated from magnetic field measurements and are found to flow in toroidal vortices. [S0031-9007(99)08772-4]

PACS numbers: 52.35.Bj, 52.35.Hr, 52.40.Db

Alfvén waves are known to be very important in the dynamics of magnetized plasmas in space and in laboratories on earth [1]. They transport electromagnetic energy, may accelerate plasma particles, and are produced in large, dense, magnetized laboratory plasmas or in almost any space plasma environment where there are changes in plasma currents or magnetic field configuration. The experiments described in this Letter are concerned with the shear mode of the Alfvén wave launched from sources with transverse scale comparable to the electron collisionless skin depth, δ $(= c/\omega_{\rm pe})$. The shear wave propagates at frequencies below the ion cyclotron frequency $(\omega_{\rm ci})$, and the associated currents are divergenceless $(\nabla \cdot \mathbf{j} = 0)$ with the currents parallel to the background magnetic field, $\mathbf{B}_0$, carried by electrons while ions carry the currents transverse to the field through the polarization drift.

In a plasma where the ion temperature is much smaller than the electron temperature $(T_i \ll T_e)$ as is typical of the Large Plasma Device (LAPD) discharge plasma, the dispersion relation for shear Alfvén waves is [2]

$$Z'(\zeta)[s^2(1 - \bar{\omega}^2) - \zeta^2] = k_\perp^2 \delta^2, \qquad (1)$$

where $s = v_A/v_e$ is the ratio of the Alfvén velocity $[v_A = (B_0^2/4\pi n m_i)^{1/2}]$ to the electron thermal speed, $v_e = (2T_e/m_e)^{1/2}$ with m_e the electron mass, $\bar{\omega}$ is the normalized angular frequency $(\bar{\omega} = \omega/\omega_{\rm ci})$, and where $Z'(\zeta)$ is the derivative of the plasma dispersion function [3] with respect to ζ with $\zeta = \omega/k_\parallel v_e$. The parameter s^2 is related to the electron plasma beta, $\beta_e = 8\pi n_e T_e/B_0^2$, as

$$s^2 = \frac{v_A^2}{v_e^2} = \frac{m_e}{m_i}\frac{1}{\beta_e}. \qquad (2)$$

While, for the experiments reported here, Eq. (1) must be used to describe the propagation of the shear Alfvén wave, there are two limiting cases that simplify the dispersion relation and illuminate the behavior of the wave. These two limiting cases are the inertial Alfvén wave when $s^2 \gg 1$, and the kinetic Alfvén wave when $s^2 \ll 1$. For the inertial Alfvén wave, the asymptotic expansion of the derivative of the plasma dispersion function can be used $(Z' = 1/\zeta^2)$ and Eq. (1) gives

$$\frac{\omega^2}{k_\parallel^2} = \frac{v_A^2(1 - \bar{\omega}^2)}{(1 + k_\perp^2\delta^2)};$$
$$\frac{v_{g\perp}}{v_A} = -(k_A\delta)\frac{k_\perp\delta(1 - \bar{\omega}^2)}{1 + k_\perp^2\delta^2} \qquad (v_A^2 \gg v_e^2), \qquad (3)$$

where $k_A = \omega/v_A$ and $v_{g\perp}$ is the perpendicular group velocity. For the case $k_\perp = 0$, the dispersion relation is the standard MHD dispersion relation and the perpendicular group velocity is zero. The inertial Alfvén wave is a backward wave for propagation across the magnetic field (i.e., the sign of the group velocity is opposite the sign of $k_\perp$). For the kinetic Alfvén wave, ζ is small and $Z' \approx -2$, and Eq. (1) gives

$$\frac{\omega^2}{k_\parallel^2} = v_A^2(1 - \bar{\omega}^2 + k_\perp^2\rho_s^2);$$
$$\frac{v_{g\perp}}{v_A} = (k_A\rho_s)\frac{k_\perp\rho_s}{1 + k_\perp^2\rho_s^2} \qquad (v_A^2 \ll v_e^2), \qquad (4)$$

where ρ_s is the ion sound gyroradius, $\rho_s = c_s/\omega_{\rm ci}$, with $c_s = (T_e/m_i)^{1/2}$ the ion sound speed. Once again the standard MHD dispersion relation is recovered in the case $k_\perp = 0$, but now the wave is a forward wave for propagation across the magnetic field.

The inclusion of nonzero $k_\perp$ values, in particular $k_\perp$ values with $k_\perp\delta \approx 1$, in the propagation of the shear Alfvén wave has important consequences for space and laboratory plasmas. Field-aligned current filaments with δ transverse size have been observed in space plasmas [4]. Such structures may also naturally occur at the edge of magnetic confinement devices for fusion applications and other laboratory plasmas [5]. Skin-depth size sources are predicted [6] and have been observed [7] to produce profound effects on the radiation pattern. In particular, the spreading of wave energy across the magnetic field and the transition from forward to backward wave from the kinetic to inertial regime affects the phenomena of field line resonance [8]. Bellan [9] has suggested that cross-field propagation destroys the field line resonance, while

Streltsov *et al.* [10] suggest that the transition from kinetic to inertial wave along field lines in the magnetosphere, in fact, leads to an energy focusing and results in a localized field line resonance structure that creates the curtainlike geometry of auroral arcs. This Letter reports the first direct observation of the kinetic shear Alfvén wave in the regime with $k_\perp \delta \approx 1$, and the first confirmation of the transition from forward to backward propagation in the transition from the kinetic to inertial Alfvén regimes.

The experiments were conducted in the LAPD [11] at the University of California, Los Angeles. A schematic diagram of the experiment is presented in Fig. 1. The LAPD's vacuum vessel has an overall length of 11 m. At one end sits an electron beam source which consists of a BaO coated cathode and a wire mesh anode. The accelerated electrons ionize He gas producing a highly ionized plasma. The plasma used in these experiments is 36 cm (at least 150 ion gyro-radii) in diameter and 9.4 m (about four parallel Alfvén wavelengths) long. The LAPD is capable of producing a background magnetic field strength, $B_0 \leq 2.5$ kG and He plasmas with density $n_e \leq 5 \times 10^{12}$ cm^{-3} and electron temperature $T_e \leq 15$ eV. In the experiments to be described, the propagation of the shear Alfvén wave launched from a disk antenna producing waves with $k_\perp \delta \approx 1$ is studied as the value of the electron beta is varied from several times greater than the mass ratio (the kinetic regime) to several times smaller than the mass ratio (the inertial regime). The parameters B_0, n_e, and T_e are varied to produce changes in the electron beta but are limited to the range $0.7 \leq B_0 \leq 2.0$ kG, $1.4 \times 10^{12} \leq n_e \leq 2.4 \times 10^{12}$ cm^{-3}, and $1.3 \leq T_e \leq 11$ eV. Diagnostics for this experiment include a radio frequency magnetic field probe, Langmuir probe, and a 70 GHz microwave interferometer for calibrated plasma density measurements.

Shear Alfvén waves are launched using an antenna which is constructed from two identical 50% transparent wire mesh disks with radius $a = 0.5$ cm. The electron skin depth, δ, in the experiments ranges from 0.34 to 0.45 cm so that $1.1 < a/\delta < 1.5$. The disk surface normals are oriented parallel to $\mathbf{B}_0$, and they are electrically insulated from each other and separated by 0.1 cm. The disks are connected to a coaxial cable in which each conductor services one disk and current is fed to the disks 180° out of phase. The ac component of the current flows in the plasma as modulated plasma electron flux. The wave frequency, ω, is typically $0.64\omega_{ci}$, and the parallel wave length, $\lambda_\parallel$, is about 2.5 m.

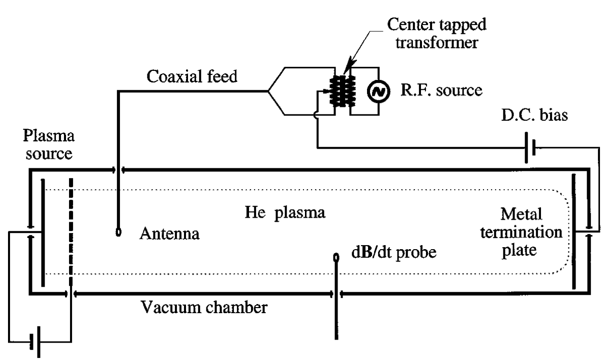

FIG. 1. During the experiment, the termination plate is at plasma floating potential; the dc bias holds the disks up near the plasma potential while the rf source drives the oscillating current.

The time derivative of the wave magnetic field, $d\mathbf{B}/dt$, is detected using a triaxial arrangement of induction coils. The decay length of the waves launched by the antenna is short enough that reflections from the ends of the machine are insignificant. A single frequency, steady state, radiation pattern is measured in several planes perpendicular to $\mathbf{B}_0$. The radiation is observed to be azimuthally symmetric, and the field data are averaged over azimuth and viewed as a function of r and z, where r is the transverse distance from the axis of symmetry of the radiation pattern and z is the axial distance from the antenna.

Since the wave energy radiated from the disk source is propagating outward, Eq. (4) indicates that the forward propagating kinetic wave should exhibit outward radial phase propagation (i.e., in the positive r direction). In contrast, Eq. (3) indicates that the backward propagating inertial wave should exhibit inward radial propagation. Figure 2 shows the measured wave phase as a function of radius, $\phi(r)$, for both an inertial ($\beta_e m_i/m_e = 0.23$) and a kinetic ($\beta_e m_i/m_e = 6.8$) wave; a negative slope indicates a radially backward wave. The change from forward to backward propagation as the electron beta crosses the mass ratio is demonstrated by the change from increasing phase with increasing r of the $\beta_e m_i/m_e = 6.8$ case to the decreasing phase with increasing r of the $\beta_e m_i/m_e = 0.23$ case.

Figure 2 also shows radial profiles of the magnitude of the azimuthal component, $|B_\theta|$, of the wave magnetic field for the kinetic wave. The radial structure of the magnitude of the magnetic field of shear Alfvén waves launched from small sources is predicted to exhibit multiple peaks, and, as z increases, so does the number of peaks in the radial structure (assuming very small damping). The origin of these peaks is subtle and too involved to discuss here. Basically, they arise from interference effects as discussed in the papers by Morales *et al.* [6]. However, at sufficiently small z and for all values of β_e, these waves exhibit a single peak in $|B_\theta(r)|$, which we call the main peak [see Fig. 2(a)]. The radial profile rises linearly from the symmetry axis (at $r = 0$), peaks, and then decreases monotonically. At larger axial distances, secondary peaks appear at different radial positions depending on whether the shear wave is in the inertial or kinetic regime. A signature feature of the kinetic wave, predicted by theory, is a secondary peak at a radial position smaller than the main peak. Such a peak is observed for the case $\beta_e m_i/m_e = 6.8$ as shown in Figs. 2(b) and 2(c). The peaks

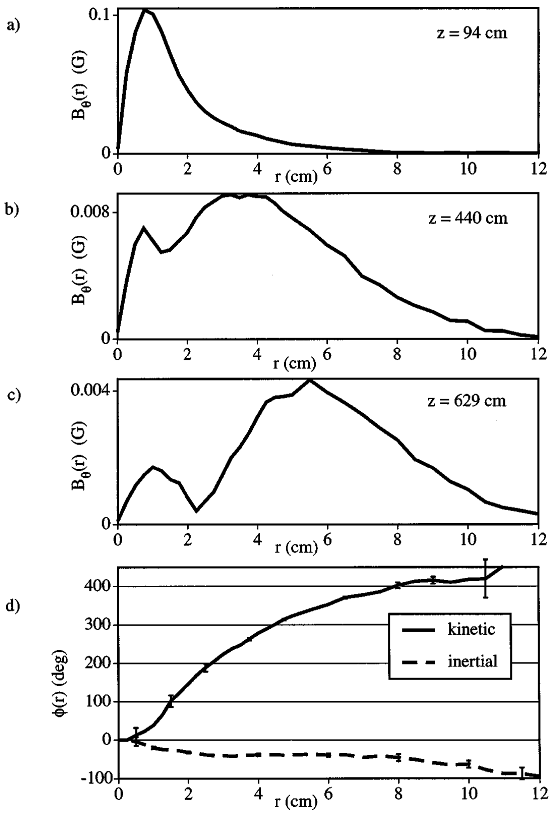

FIG. 2. (a), (b), and (c): $|B_\theta(r)|$ for the case with $\beta_e m_i/m_e = 6.8$ at several z positions. $|B_\theta(r)|$ is the amplitude of the azimuthal component of the wave magnetic field. (d) Phase of B_θ as a function of r, $\phi(r)$. The solid line is for the case with $\beta_e m_i/m_e = 6.8$ (at $z = 440$ cm), and the dashed line is for the case with $\beta_e m_i/m_e = 0.23$ (at $z = 189$ cm; amplitude profile not shown).

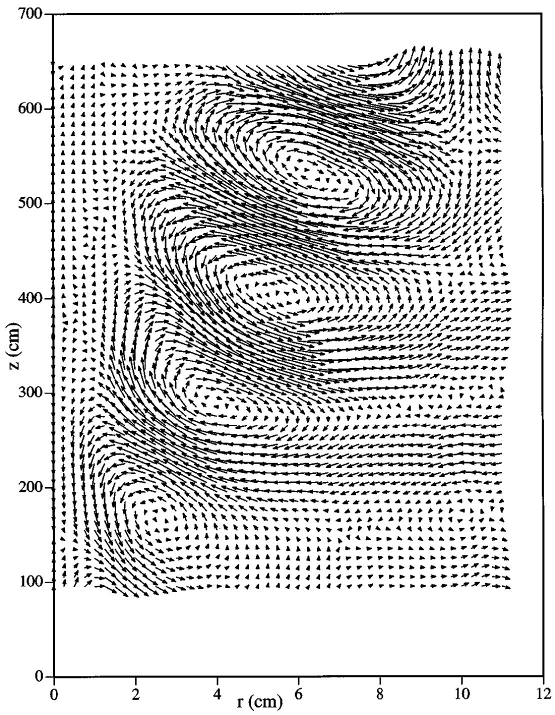

FIG. 3. The product $r\mathbf{j}(r,z)$ is presented at an instant of time. $\mathbf{j}$ is calculated for the case with $\beta_e m_i/m_e = 6.8$. The source is located at $z = 0$, $r = 0$, and has a 0.5 cm radius. The centers of the vortices are located 1.25 m or $\lambda_\parallel/2$ apart.

appearing at $r = 0.7$ in Fig. 2(b) and at $r = 1.0$ cm in Fig. 2(c) are the secondary peaks expected for the kinetic shear wave.

The current density derived from the measured magnetic field using the relation, $\mathbf{j} = (\nabla \times \mathbf{B})/\mu_0$ provides some insight into the structure of the shear wave radiated from the small source. The current vector field, $\mathbf{j}(\mathbf{r})$ is azimuthally symmetric without any azimuthal component and is efficiently represented as vectors in the r, z plane, $\mathbf{j}(r,z)$. The current structure includes radial polarization currents which flow out from and into a core of axial current. Because the magnitude of these radial currents decreases radially at least as fast as $1/r$, the quantity $r\mathbf{j}(r,z)$ is presented in Fig. 3 [12]. Showing this vector field rather than $\mathbf{j}(r,z)$ allows the radial currents to be easily seen at larger radii. Several features are evident in Fig. 3. The structure is radially larger at greater distances from the source, and clearly illustrates that Alfvén wave energy radiated from skin-depth size sources spreads across the ambient magnetic field. The measured angle of spreading is 0.6° which agrees well with the theoretically predicted value of 0.55°. The multiple vortices in the r, z plane represent successive toroidal cells of poloidal current. The toroids are stacked half a wavelength apart with their symmetry axes aligned along the z axis. The direction of the poloidal current reverses in successive cells. Outward radial currents return to the core via axial currents at rather small values of r (between 5 and 10 cm). This behavior causes the azimuthal magnetic field amplitude to decrease faster than $1/r$. This rapid falloff arises from the design of the two-disk antenna. Simulation of radiation from single-disk antennas does not exhibit these axial return currents.

In summary, we have observed the transition from forward to backward propagation in the shear Alfvén wave as the plasma electron beta transits the mass ratio, the identifying secondary peak at small radius of the kinetic Alfvén wave, and the details of the radiated current pattern of the kinetic Alfvén wave. The radial phase velocity was observed to exhibit a sign reversal in the transition from the kinetic to the inertial regimes where the inertial wave is a radially backward wave. In the most kinetic case studied (where $\beta_e m_i/m_e = 6.8$), the observed wave exhibited a secondary peak structure in the radial profile of $|B_\theta|$ characteristic of the kinetic limit. The wave currents launched by the two-disk antenna as calculated from the wave magnetic field data were found to circulate in toroidal vortices that spread across the magnetic field as the distance from the source increased. These results are relevant to and should contribute to the understanding of spacecraft observations. Recent observations from the Freja and FAST satellites show that skin-depth scale current structures abound in space, and they are frequently observed in conjunction with Alfvénic magnetic and electric field fluctuations.

Funding was provided by ONR, NSF-ATM, and NSF-AMO. The authors gratefully acknowledge support in data acquisition, computer programming, and the development of the LAPD itself by S. Rosenberg, S. Vincena, M. Gilmore, L. Mandrake, V. Guerrero, Z. Lucky, A. Burke, T. Tisdale, T. Drozdenko, and C. Mitchell.

[1] R.C. Cross, *An Introduction to Alfven Waves* (IOP Publishing, Bristol, England, 1988).
[2] W. Gekelman *et al.*, J. Geophys. Res. **102**, 7225 (1997).
[3] T.H. Stix, *Waves in Plasmas* (AIP Press, Woodbury, New York, 1992), pp. 202–210.
[4] J.P. McFadden *et al.*, J. Geophys. Res. **95**, 6533 (1990); W. Borovsky, J. Geophys. Res. **98**, 6101 (1993); H. Lühr *et al.*, Geophys. Res. Lett. **21**, 1883 (1994); R. Lundin *et al.*, Geophys. Res. Lett. **21**, 1903 (1994).
[5] B.D. Fried *et al.*, Bull. Am. Phys. Soc. **36**, 2499 (1991).
[6] G.J. Morales, R.S. Loritsch, and J.E. Maggs, Phys. Plasmas **1**, 3765 (1994); G.J. Morales and J.E. Maggs, Phys. Plasmas **4**, 4118 (1997).
[7] M. Ono, Phys. Rev. Lett. **42**, 1267 (1979); G.G. Borg *et al.*, Plasma Phys. Controlled Fusion **27**, 1125 (1985); H. Weisen *et al.*, Phys. Rev. Lett. **63**, 2476 (1989); W. Gekelman, D. Leneman, J. Maggs, and S. Vincena, Phys. Plasmas **1**, 3775 (1994); W. Gekelman, S. Vincena, and D. Leneman, Plasma Phys. Controlled Fusion **39**, A101 (1997); D. Leneman, doctoral thesis, UCLA, 1998.
[8] D.J. Southwood, Planet. Space Sci. **22**, 483 (1974); J.C. Samson *et al.*, J. Geophys. Res. **101**, 17 373 (1996).
[9] P.M. Bellan, Phys. Plasmas **1**, 3523 (1994).
[10] A.V. Streltsov *et al.*, J. Geophys. Res. **103**, 26 559 (1998).
[11] W. Gekelman *et al.*, Rev. Sci. Instrum. **62**, 2875 (1991).
[12] A dynamic version can be viewed at the laboratory's web site: http://plasma.physics.ucla.edu/lapd.